Development and application of perovskite-based catalytic membrane reactors

S. Irusta [*], M.P. Pina, M. Menéndez and J. Santamaría [**]

Department of Chemical and Environmental Engineering, University of Zaragoza, 50009 Zaragoza, Spain
E-mail: iqcatal@posta.unizar.es

Received 5 March 1998; accepted 3 June 1998

The preparation and characterization of catalytic membranes containing La-based perovskites are reported. The membranes were prepared by *in situ* crystallization of different perovskites inside a porous α-alumina matrix. Preponderance of the Knudsen-diffusion regime during membrane operation was obtained with perovskite loads of 2 wt% and higher. The catalytic membranes obtained were used as combustors of VOCs (toluene and methyl ethyl ketone) contained in air streams, at concentrations between 875 and 3450 ppmV, and space velocities of up to 27200 h^{-1}. The membranes were operated in the flow-through mode, which resulted in total VOC combustion at moderate temperatures.

Keywords: catalytic membranes, perovskites, VOC combustion

1. Introduction

Research in the field of catalytic membrane reactors is aimed to exploiting the opportunities that the combination of catalysts and membranes provide, regarding new modes of contact, integration of reaction + separation and unconventional heat and mass transfer arrangements. With catalytic membranes, the reaction (or at least part of it), takes place directly on the membrane. Porous ceramic membranes can be made out of a variety of materials such as alumina, silica, titania, zirconia, zeolites... All of these can have catalytic activity under suitable operating conditions. If enough activity and selectivity can be obtained directly from the membrane constituent material, then no further processing is necessary, and the objective of membrane preparation is solely to ensure that mechanical and permeation requirements are met. Thus Zaspalis et al. [1] prepared a thin γ-alumina membrane by slip casting on top of an α-alumina support, and obtained a membrane that was active for the oxidative dehydrogenation of methanol to formaldehyde.

On the other hand, when the membrane is not catalytically active under reaction conditions, an active phase can be deposited on it, using the membrane material as a support. Impregnation, ion-exchange, chemical vapour deposition (CVD), and sol–gel techniques are commonly employed for this purpose. Regarding this point, most of the differences with the use of the same techniques in conventional catalyst preparation stem from the existence of a continuous porous membrane structure. Thus, active materials (e.g., Pt) can be deposited on asymmetric porous membranes, with or without modification of the membrane by deposition of γ-alumina, e.g., [2–4]. In this case, different active phase distributions can be obtained by impregnation from one or from both sides, by previously filling the pores with an inert liquid or by allowing the membrane to dry from one or from both sides. Pt/γ-alumina membranes have also been prepared by CVD, by making the organic precursor flow across the porous membrane structure [5]. Again, the properties of the continuous porous structure play an important role: the residence time of precursor molecules and the deposition temperature can be tailored to obtain a homogeneous deposition or, if desired, a sharp step distribution of the active component.

Successive deposition of inert and/or active layers using sol–gel techniques can also give non-uniform radial distributions of active components. This approach was successfully employed by Yeung et al. [6] to vary the position of a narrow step distribution of Pt across the membrane radius. Along this line, Michaels [7] suggested the possibility of placing consecutive ceramic layers of different materials via sol–gel, where each layer could be loaded with a different catalyst. Another possible method to obtain a non-uniform catalyst distribution involves the reaction of suitable precursors, which are fed from opposite sides of the membrane structure. An example of this approach is the work of Gavalas et al. [8], who used the reaction between SiH_4 and oxygen at 450 °C to deposit silica within the walls of porous substrates.

The objective of this work was to obtain a perovskite-loaded membrane that could be used as a catalytic combustor. In this case, a homogeneous distribution of the perovskite catalyst throughout a thermally stable support structure (α-alumina) was sought. The approach followed was to fill the pores of the membrane structure with appropriate perovskite precursors, which can then be forced

---

[*] To whom correspondence should be addressed.
[**] On leave of absence from INCAPE, Argentina.

to react in a confined environment. The resulting membranes have been tested in the catalytic combustion of toluene and methyl ethyl ketone (MEK), as examples of volatile organic compounds (VOCs). In previous works [4,5], it was shown that Pt-loaded, flow-through catalytic membranes working in the Knudsen-diffusion regime performed as efficient VOC combustors. The mode of contact, which is important in any catalytic system, can be considered critical for VOC combustion processes, where reactant concentrations are measured in the ppm range. The contactor used in these works, a flow-through membrane with a premixed gas feed stream, departed considerably from the usual catalytic membrane configuration for oxidation reactions, which consists of a catalytic membrane where reaction takes place with reactants fed from opposite sides. In the present work, the feasibility of using flow-through, perovskite-based ceramic membranes for the complete combustion of VOCs has been investigated. To this end, different active phases ($LaMnO_3$, $LaCoO_3$, $La_{0.8}Sr_{0.2}MnO_{3-x}$ and $La_{0.8}Sr_{0.2}CoO_{3-x}$), have been deposited onto a preexisting membrane structure.

2. Experimental

The membranes were prepared from commercial microfiltration tubes (SCT). The starting material was 1.5 mm thick, 10 mm o.d. asymmetric ceramic (α-alumina) tubes, with a separation layer where the limiting pores had a diameter of 200 nm.

The preparation of perovskite oxides involves a solid state reaction of the precursor oxides to form the characteristic ABO_3 structure. This requires significant exposure times at high temperatures, leading to a low specific surface of the catalyst. In order to increase the surface area of the perovskites, a number of different precursor salts have been used, including glycolates, carbonyls, citrates and oxalates. We have used the so-called citrates method, as described by Taguchi et al. [9], who reported the formation of perovskites at temperatures between 300 and 900 °C.

The perovskites prepared using the citrates method were $LaMnO_3$, $LaCoO_3$, $La_{0.8}Sr_{0.2}MnO_{3-x}$ and $La_{0.8}Sr_{0.2}CoO_{3-x}$. For simplicity, these will be denoted as La–Mn, La–Co, La–Sr–Mn and La–Sr–Co in the remainder of this work. The salts used were initially nitrates, each of which (La, Mn, Co, Sr), was dissolved in deionized water. After titration, the solutions were mixed in the desired proportions and N moles of citric acid were added (N being equal to the total number of moles of La and Sr, Co or Mn). The membrane was impregnated with the solution, then dried for 12 h at 100 °C, and calcined in two steps, 30 min at 300 °C followed by 2 h at 600 °C or 6 h at 800 °C. This allowed the formation of perovskite structure within the membrane, as confirmed by XRD analysis. Often, in order to achieve the desired weight increase, several successive cycles, each involving impregnation drying and calcination steps were required.

X-ray diffraction (XRD) analysis was carried out with an Rigaku/Max System diffractometer using Ni-filtered Cu Kα radiation and a graphite monochromator between 5 and 80° at a scan rate of 0.02°/s, except in some measurements in which a slower rate of 0.25°/min was used. The membrane texture and the appearance of perovskite deposits were examined by SEM (JEOL JSM 6400), in transversal cuts, where the radial distribution of perovskite could also be determined by electron-probe microanalysis (EPMA).

BET surface areas were determined using a dynamic Micromeritics (Chemisorb 2700) equipment. Pore volume and pore size distribution were characterized by mercury intrusion porosimetry (Autopore II 9220, Micromeritics). The permeation characteristics of the membrane were determined by measuring nitrogen permeation rates at room temperature, using an automated gas permeation cell in which the total pressure and the pressure differential across the membrane were accurately controlled. The permeation flux (in mol/m^2 s bar), changes with the average pressure in the membrane according to [10]

$$F = 1.06\frac{\varepsilon r}{L\tau\sqrt{MRT}} + 0.125\frac{\varepsilon r^2}{L\tau\mu RT}P_{\text{av}} = \alpha + \beta P_{\text{av}},$$

where F is the permeation flux normalised per unit of time, area and pressure difference (mol/m^2 s bar), P_{av} is the average pressure across the membrane (bar), μ the viscosity, T the absolute temperature and R the universal gas constant. L, ε, τ and r are respectively the membrane thickness, porosity, tortuosity and pore radius. α and β indicate respectively the Knudsen and laminar contributions to the permeation flux. A good linear fit of F vs. P_{av} was obtained with all the membranes tested in this work.

Catalytic tests were carried out in a stainless steel membrane module described previously [5]. The experimental system is shown in figure 1. It consisted of (1) a feed section in which a mass-flow-controlled (Brooks) air stream was saturated with the selected organic compound and mixed with a second mass-flow-controlled air stream to give the desired final concentration, and (2) a reaction section with the catalytic membrane module inside an electric furnace. Saturation was achieved in the feed section by using a sintered glass frit to bubble the air stream through a series of three flasks containing the desired VOC, the first at room temperature and the other two immersed in an ice bath. This resulted in a very stable partial pressure of the VOC at the exit of the saturation train. Both, toluene and methyl ethyl ketone (MEK), were used as representative of aromatic and oxygenated VOCs respectively. The volatile organic compounds could be fed to the reactor alone or in a binary mixture, in which case a duplicate saturation system was used. The feed mixture entered the membrane tube side and then permeated across the membrane wall. The combustion was essentially complete, with a CO/CO_2 ratio at the light-off temperature which was typically in the region 1/80 to 1/200 for La–Co, and 1/20 to 1/30 for La–Mn perovskites. Other oxidation products were not observed. The combustion temperatures re-

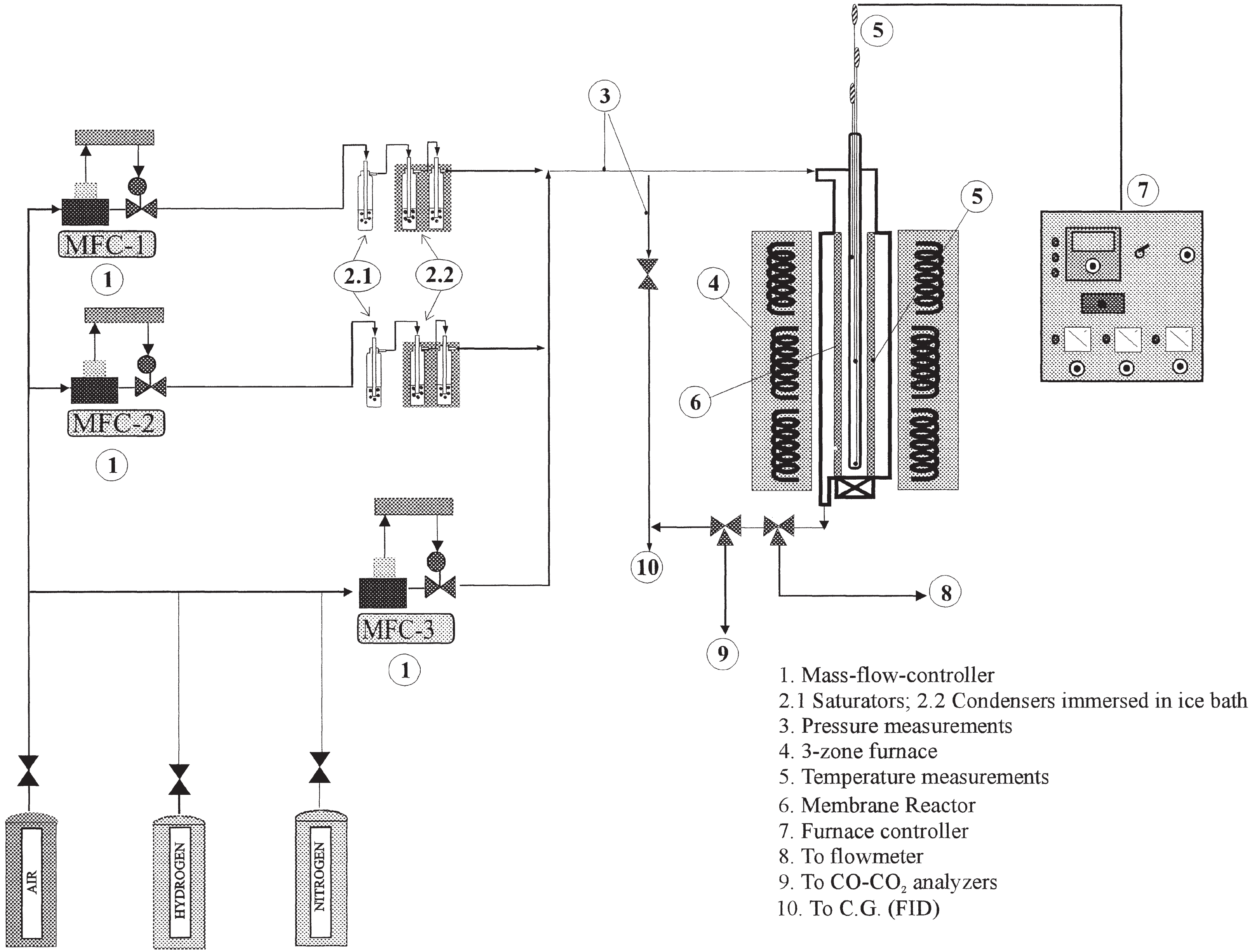

Figure 1. Experimental set up for the reaction experiments.

Table 1
Some characteristics of the perovskite membranes prepared.

Composition	Perovskite loading (%)	S_{BET}[d] (m^2/g)	S_{BET}[e] (m^2/g)	S_{BET}[f] (m^2/g)	% Knudsen contribution[g]	Permeation flux (cm^3 N_2/cm^2 min)
[a]La–Co	3.4	0.15	0.15	3.0	76	453.8
[a]La–Co	6.6	0.18	0.6	3.0	75	398.6
[a]La–Sr–Co	3.9	0.68	13.6	10.0	–	–
[a]La–Mn	2.5	0.43	11.2	12.9	83	412.7
[a]La–Mn	4	–	–	12.9	85	279.5
[a]La–Mn	6.0	–	–	12.9	84	211.4
[a]La–Mn	7.8	–	–	12.9	72	117.9
[a]La–Sr–Mn	4.5	0.51	7.8	18.6	–	–
[b]La–Co	5.8	1.21	18.7	12.0	–	–
[b]La–Sr–Co	1.6	0.37	13.9	13.0	70	498.2
[b]La–Sr–Co	6.8	1.12	14.7	13.0	69	211.6
[b]La–Sr–Co	8.3	1.59	17.5	13.0	78	127.3
[b]La–Sr–Mn	2.7	–	–	32.1	64	367.4
[b]La–Sr–Mn	4.4	1.22	24.9	32.1	–	–
[c]La–Sr–Mn	6.1	0.74	9.8	32.1	–	284.0

[a] Calcined at 800 °C for 6 h; [b] Calcined at 600 °C for 2 h; [c] Calcined at 600 °C for 4 h.
[d] Per gram of membrane; [e] Per gram of perovskite.
[f] BET surface area of bulk perovskite crystals, prepared by the same method.
[g] Estimated at an average pressure of 1 bar.

Table 2
Light-off and total (99%) combustion temperatures for toluene and MEK on different perovskite membranes.

Type of perovskite	Perovskite loading (%)	Calcination temp. (°C)	VOC	Concentration (ppmV)	Space velocity[a] (h^{-1})	$T_{50\%}$[b] (°C)	$T_{99\%}$[b] (°C)
La–Co	6.6	800	toluene	2225	7200	325	410
La–Mn	6.0	800	toluene	1750	10000	342	397
La–Co	5.8	600	MEK	1700	10000	271	290[c]
La–Sr–Co	6.8	600	MEK	2300	10000	270	330[c]
La–Mn	6.0	800	MEK	1800	9200	288	324
La–Sr–Mn	6.1	600	MEK	1500	10000	279	303
La–Sr–Mn	6.1	600	MEK	1400	27200	311	334

[a] Total flow rate divided by the volume corresponding to the permeable section of the membrane wall, inside which the catalyst is located.
[b] Temperatures for VOC conversions of 50 and 99%, respectively.
[c] Temperature for VOC conversion of 95%.

ported below correspond to the reading of a thermocouple directly in contact with the membrane wall. After passing through the membrane, the exit stream was directed to an on-line gas chromatograph (HP5890, FID detector), and to CO and CO_2 analysers (Sensotran). In some experiments, instead of the analysers a methanator reactor (60 wt% Ni/Al_2O_3) was used after the separation column and before the FID detector, to convert CO and CO_2 into methane.

3. Results and discussion

3.1. Membrane characterization

The membrane permeation characteristics and BET area measurements are given in table 1. It can be seen that the calcination temperature has a strong influence on the surface area of the perovskites synthesised: the BET areas per gram of perovskite given in table 1 for samples calcined at 600 °C are considerably larger than for those calcined at 800 °C, irrespective of whether bulk or membrane-supported samples are compared. Also, for the samples calcined at 800 °C, the specific surface area per gram of perovskite is in most cases lower when the perovskite was incorporated into the membrane structure, compared to its value as unsupported bulk crystals. This is due to the extended exposure at higher temperatures when the perovskites were deposited inside the membrane structure, since, as noted above, several impregnation + calcination cycles were necessary to achieve the desired perovskite loading. At 600 °C this extended exposure is less detrimental, and table 1 shows that the surface areas for bulk and supported samples are similar.

Regarding the permeation regime, for all the membranes tested, the percentage of Knudsen contribution remains in a relatively narrow range (around 20 percentage points), in spite of a five-fold variation in the perovskite load. This seems to indicate that the controlling pore diameter for permeation does not change with successive incorporations of

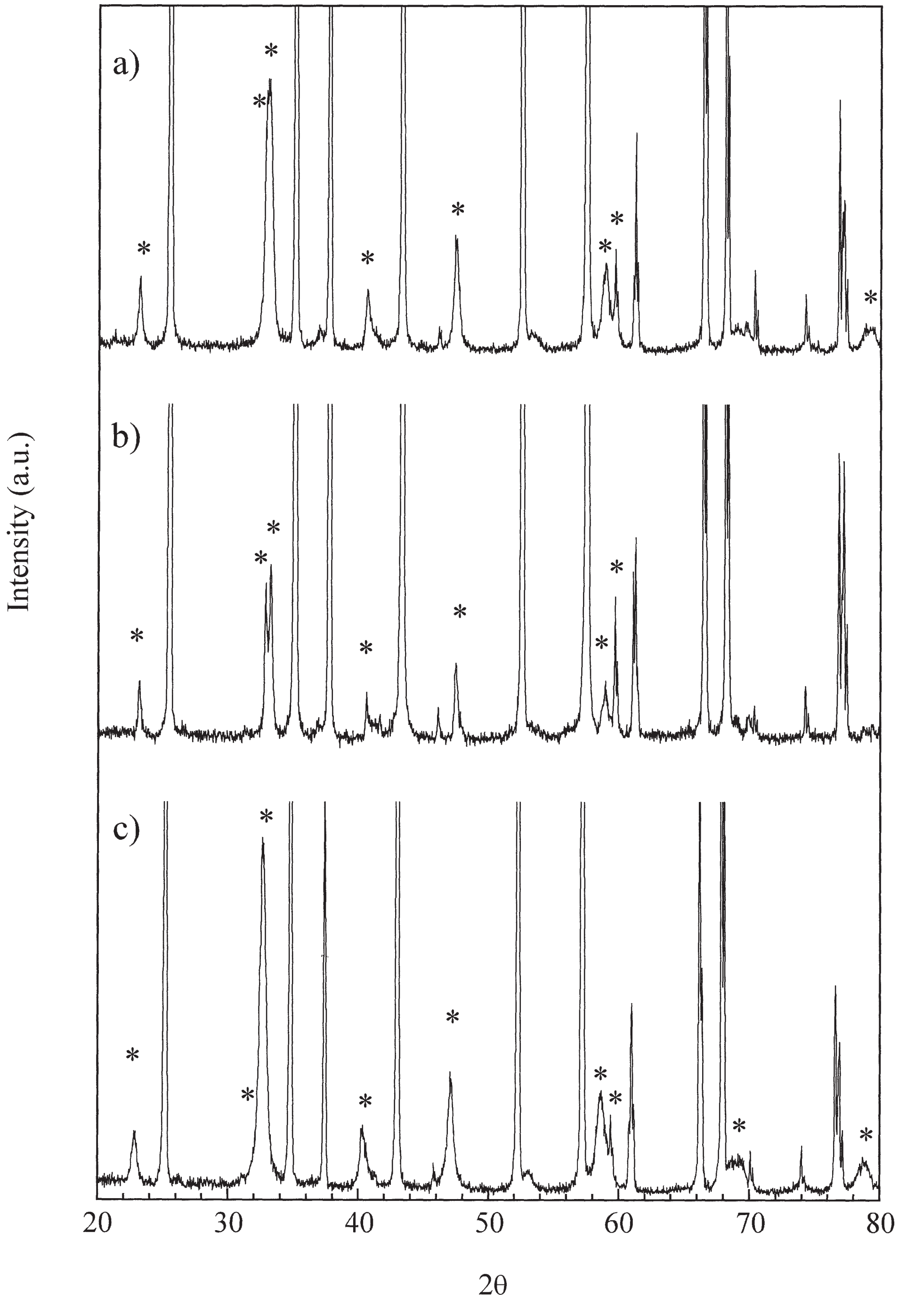

Figure 2. XRD patterns for different perovskite membranes: (a) La–Co (5.8 wt%), calcined at 600 °C; (b) La–Co (1.5 wt%), calcined at 800 °C; (c) La–Sr–Co (6.8 wt%), calcined at 600 °C.

active material. As could be expected, for all the membranes tested the permeation data (not shown) indicated a consistent reduction of the permeation flux as the perovskite loading was increased. However, the magnitude of this reduction depends on the particular perovskite considered: the data in table 1 show that, for instance, the permeation flux in a La–Mn membrane calcined at 800 °C with a perovskite loading of 7.8% is less than one third of the corresponding value at a perovskite loading of 2.5%; this is in contrast with the La–Co membrane, where the perovskite loading was roughly doubled (3.4 to 6.6%), with a reduction of only 12% in the permeation flux.

The results of XRD analysis are shown in figure 2 (membranes loaded with La–Co and La–Sr–Co perovskite precursors), and figure 3 (La–Mn and La–Sr–Mn), after calcination at 600 °C to form the perovskite. In the case of the La–Co perovskite, XRD analysis of the membrane calcined at 800 °C is also shown for comparison purposes. It can be seen that the formation of perovskites inside the membrane structure occurs readily at 600 °C, and the process is

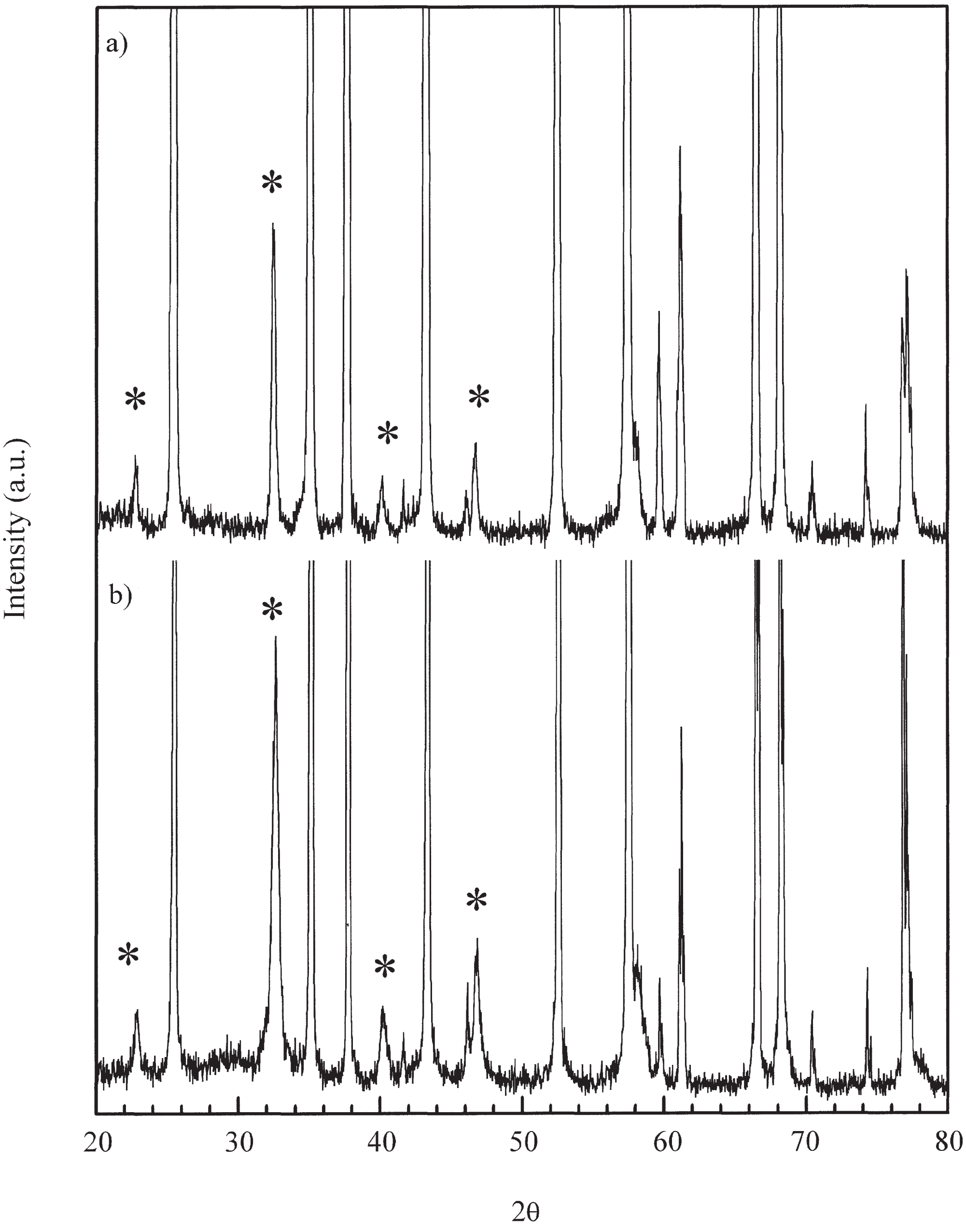

Figure 3. XRD patterns for different perovskite membranes: (a) La–Mn (5.9 wt%) and (b) La–Sr–Mn (4.4 wt%), both calcined at 600 °C.

enhanced by calcination at 800 °C (note the different perovskite loadings used). A major concern regarding the synthesis of perovskite crystals inside the pores of the α-Al_2O_3 membrane was the possible formation of aluminates such as $CoAl_2O_4$, or Al-containing perovskites such as $LaAlO_3$. This possibility was specifically investigated in XRD patterns obtained using a lower scan rate (0.25°/min). A careful analysis of the peak positions and intensities in the XRD pattern confirmed the absence of these compounds from the membranes prepared. Similarly, the presence of segregated, single-oxide phases was not detected in the diffractograms.

SEM observations indicate that aggregates of perovskite crystals with a length of several microns are dispersed among the large α-Al_2O_3 particles that make up the support tube. Figure 4 (a) and (b) shows an example of these for the La–Co and La–Mn perovskites respectively, where it can be seen that the aggregates are composed of smaller crystal units. EPMA measurements (not shown), taken radially across the membrane showed a homogeneous distribution of the perovskite material, as could be expected given the preparation procedure employed.

3.2. Reaction experiments

Table 2 shows some of the results obtained in the combustion of toluene and methyl ethyl ketone (MEK) over catalytic membranes with perovskite loadings of around 6 wt% and higher. Note that, as stated above, the temperatures reported in the light-off curves are those measured directly on the membrane wall, and *not* the gas inlet

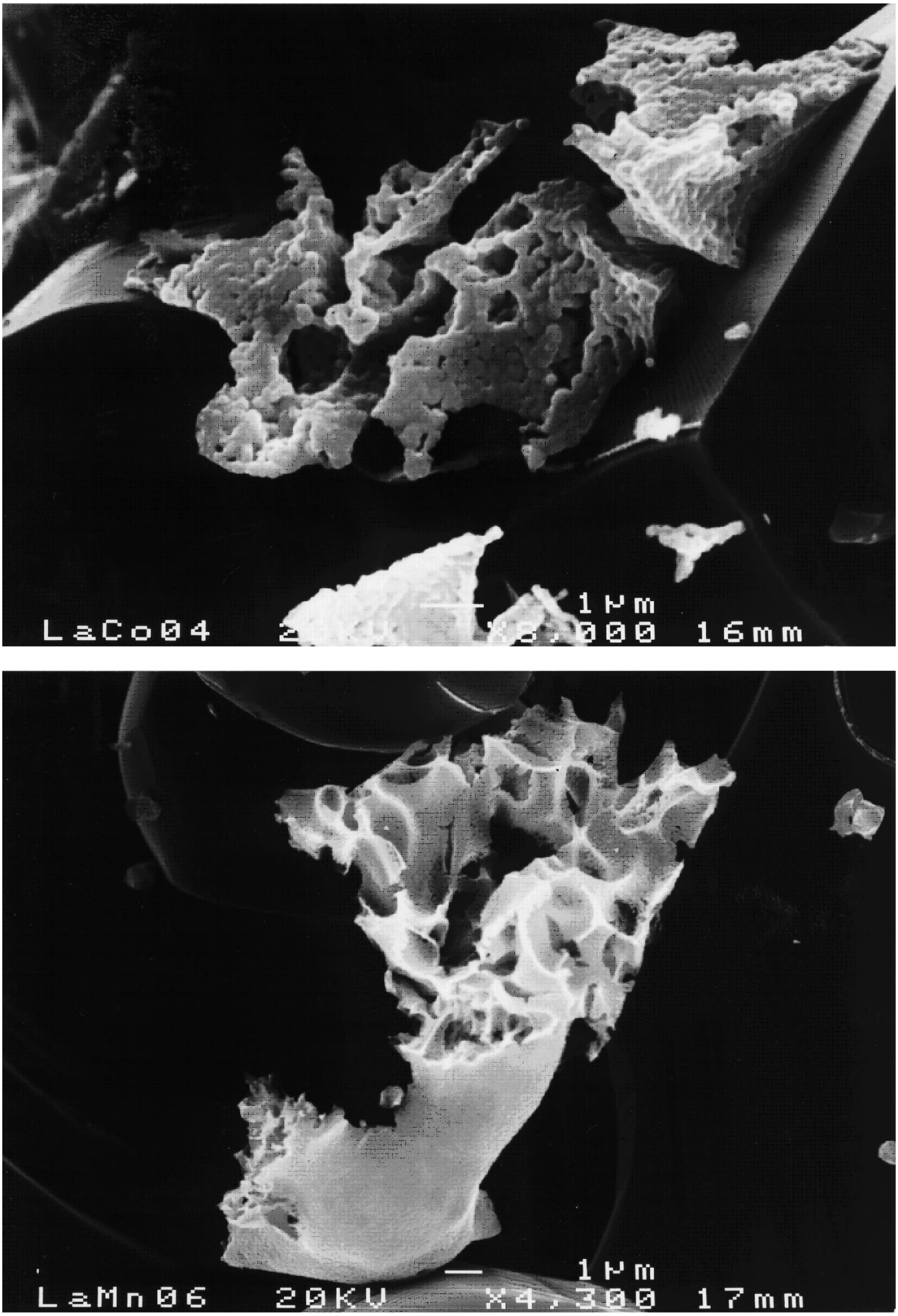

Figure 4. SEM micrographs showing transversal cuts of (a) La–Co (1.45 wt%) and (b) La–Mn (1.5 wt%) perovskite membranes.

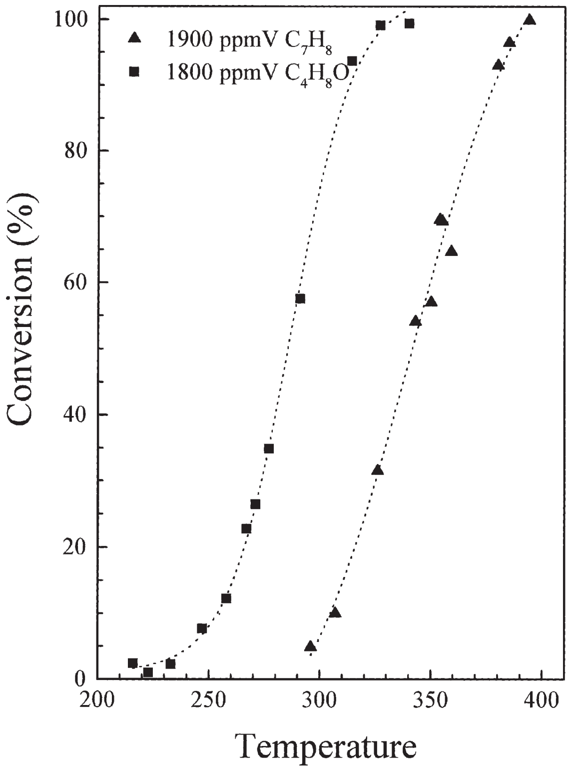

Figure 5. Light-off curves over a 6 wt% La–Mn perovskite membrane for MEK (1800 ppmV) and toluene (1900 ppmV).

temperatures. Given the exothermicity of the combustion reactions involved, the difference can be significant, except for very lean VOC streams (e.g., at a toluene concentration of 150 ppm, the differences between the inlet and exit gas temperatures, based on the adiabatic temperature rise, would be around 20 °C). It can be seen that, at these perovskite loadings, the catalytic membranes performed efficiently as VOC combustors, e.g., table 2 shows that MEK light-off and total combustion temperatures as low as 270 and 290 °C respectively were obtained, at a space velocity of 10000 h^{-1}. In addition, the membranes used were able to accommodate relatively large changes in the feed flowrate with a moderate increase in the operating temperature; e.g., for the 6.1 wt% La–Sr–Mn perovskite, a 170% increase of the feed rate translates into an increase of ca. 30 °C in the light-off and total MEK combustion temperatures. The lower light-off and total combustion temperatures for MEK in table 2 indicate that this compound is more reactive (in a molar basis) than toluene over the perovskites studied. An example of this behaviour is shown in figure 5 for the La–Mn membrane, where it can be seen that the combustion temperatures for a given conversion level are 50–60 °C lower for MEK.

The evolution of the membrane performance with perovskite loading is illustrated in figure 6 (a) and (b) for different perovskites and VOCs. The improvement with perovskite loading is evident in both figures: as the weight of perovskite incorporated onto the membrane was increased, the light-off curve consistently moved towards lower temperatures, even against a higher VOC concentration in the feed, as can be seen in figure 6b for toluene combustion. In this case, the combustion temperature decreased, in spite of the fact that the number of moles of toluene fed to the reactor increased by 112% while the perovskite load was only 94% higher. This suggests that the improvement of the combustion performance cannot be explained simply as a result of a higher space time. In fact, the probability of finding gas pathways with little or no perovskite deposits increases at low perovskite loads in a flow-through membrane reactor system. Although EPMA analysis showed a rather homogeneous distribution of perovskites across the membrane, a few connecting pores without catalyst loading would make a significant difference: since no perovskite deposits entail a lower resistance to permeation, these pores would provide preferential permeation channels, i.e., an effective bypass of perovskite deposits.

It has already been shown [4,5] that, on Pt-based catalytic membranes, the flow-through membrane combustor increases the VOC removal efficiency by lowering the mass transfer resistances involved. It should be noticed that diffusion limitations are especially significant in VOC combustion because, due to the low concentrations usually encountered, a low driving force (concentration gradient) is available. However, in the catalytic membrane system used in this work, the feed flows perpendicularly to and then across the membrane wall, thus the external film resistance is greatly reduced. With regard to the internal diffusion, a significant reduction of mass transfer resistance can be expected from forced flow under the Knudsen diffusion regime (the regime that prevails with the perovskite membranes used, as shown in table 1).

An indication of the reduction of mass transfer resistance that can be attained by the flow-through membrane reactor can be obtained by comparing its performance to that of the same membrane reactor operating as a monolith. A rough approach to monolith operation was obtained by introducing a 4 mm outside diameter quartz cylinder axially in the 7 mm internal diameter membrane tube. In this way, a 1.5 mm wide annular channel was created between the external wall of the quartz cilinder and the internal wall of the membrane. Figure 7 shows the conversion–temperature curve obtained for toluene combustion using the same membrane (6% La–Mn) in the flow-through and in the monolith operation modes. It can be seen that not only the operating temperatures required are considerably lower in the flow-through mode (about 50 °C lower for light-off and a much higher difference for total conversion), but also the shape of the curve is different. Thus, while in the flow-through operation mode a sharp increase of conversion takes place around the light-off temperature (as expected from a process under chemical kinetics control), a much slower variation with temperature can be observed for monolith operation, a clear indication of significant diffusion resistance.

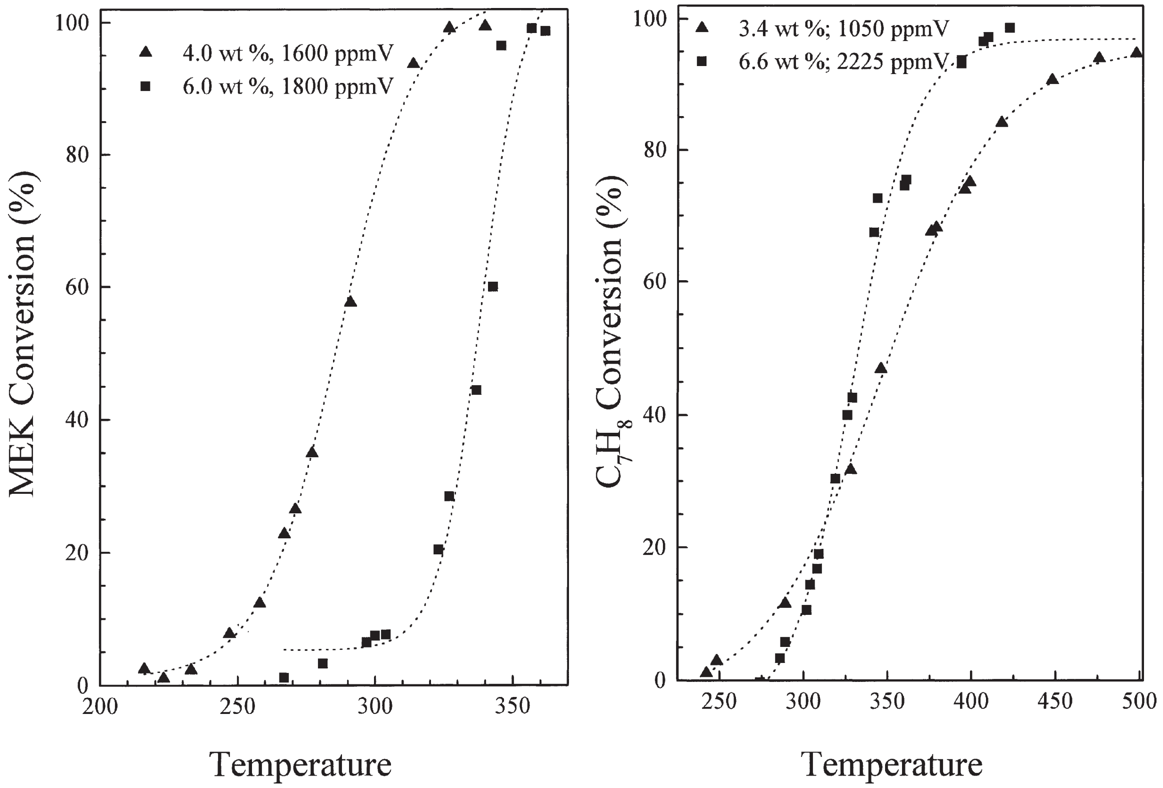

(a) (b)

Figure 6. Evolution of membrane performance with perovskite loading. (a) Light-off curves for MEK combustion; La–Mn perovskite, space velocity $= 9600\ h^{-1}$. (b) Light-off curves for toluene combustion; La–Co perovskite, space velocity $= 7450\ h^{-1}$.

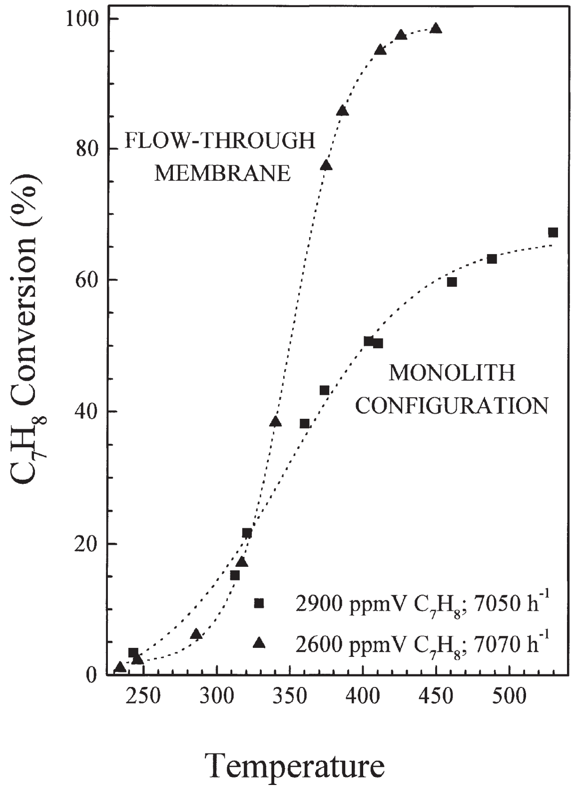

Figure 7. Conversion versus temperature curves for toluene combustion in the flow-through and in the parallel (monolith-like) operation modes. Membrane: 6 wt% La–Mn.

4. Conclusions

Perovskite-based catalytic membranes can readily be prepared by *in situ* crystallization using the appropriate precursors. The citrates method produced perovskite crystals (La–Co, La–Mn, La–Sr–Co and La–Sr–Mn) dispersed throughout the α-alumina porous structure of the membrane. The formation of aluminates or of Al-containing perovskites was not detected. The main problem with the preparation of the perovskite membranes was the low surface area obtained, especially in the membranes prepared at the higher temperatures. Ways of overcoming this difficulty by reducing the number of high temperature steps required are currently under study in our laboratory.

The perovskite-based catalytic membranes operated in the flow-through mode performed efficiently in the combustion of VOC-containing (toluene and MEK) air streams. This mode of operation gives rise to a reduction of the mass transfer resistance, which resulted in a very considerable improvement of reactor performance as compared to parallel flow (monolith-like) operation.

Acknowledgement

Financial support from DGICYT (Spain), projects (MAT95-0499 and QUI97-1085) is gratefully acknowledged. One of the authors (SI), is grateful to UNL-FOMEC (Argentina) for financial support as a postdoctoral researcher. The authors are also indebted to Dr. Olga Podyacheva, of the Boreskov Institute of Catalysis (Russia), for a useful discussion of XRD on alumina-supported perovskites.

References

[1] V.T. Zaspalis, W. van Praag, K. Keizer, J.G. van Ommen, J.R.H. Ross and A.J. Burggraaf, Appl. Catal. 74 (1991) 205.

[2] D. Uzio, J. Peureux, A. Giroir-Fendler, M. Torres, J. Ramsay and J.A. Dalmon, Appl. Catal. A 96 (1993) 83.

[3] A.M. Champagnie, T.T. Tsotsis, R.G. Minet and I.A. Webster, Chem. Eng. Sci. 45 (1990) 2423.

[4] M.P. Pina, M. Menéndez and J. Santamaría, Appl. Catal. B 11 (1996) L19.

[5] M.P. Pina, S. Irusta, M. Menéndez, J. Santamaría, R. Hughes and N. Boag, Ind. Eng. Chem. Res. 36 (1997) 4557.

[6] K.L. Yeung, R. Aravind, R.J.X. Zawada, J. Szegner, G. Gao and A. Varma, Chem. Eng. Sci. 49 (1994) 4823.

[7] A.S. Michaels, 7th ESMST Summer School, Twente University, Netherlands, 1989.

[8] G.R. Gavalas, C.E. Megiris and S.W. Nam, Chem. Eng. Sci. 44 (1989) 1829.

[9] T. Taguchi, S. Matsuura, M. Nagao, T. Choso and K. Tabata, J. Solid State Chem. 129 (1997) 60.

[10] Y.S. Lin and A.J. Burggraaf, J. Am. Ceram. Soc. 74 (1991) 219.